OPEN

Oncogene (2013) **32,** 5531–5540

www.nature.com/onc

ORIGINAL ARTICLE

S100A4 interacts with p53 in the nucleus and promotes p53 degradation

LM Orre[1], E Panizza[1], VO Kaminskyy[2], E Vernet[3], T Gräslund[3], B Zhivotovsky[2] and J Lehtiö[1]

S100A4 is a small calcium-binding protein that is commonly overexpressed in a range of different tumor types, and it is widely accepted that S100A4 has an important role in the process of cancer metastasis. *In vitro* binding assays has shown that S100A4 interacts with the tumor suppressor protein p53, indicating that S100A4 may have additional roles in tumor development. In the present study, we show that endogenous S100A4 and p53 interact in complex samples, and that the interaction increases after inhibition of MDM2-dependent p53 degradation using Nutlin-3A. Further, using proximity ligation assay, we show that the interaction takes place in the cell nucleus. S100A4 knockdown experiments in two p53 wild-type cell lines, A549 and HeLa, resulted in stabilization of p53 protein, indicating that S100A4 is promoting p53 degradation. Finally, we demonstrate that S100A4 knockdown leads to p53-dependent cell cycle arrest and increased cisplatin-induced apoptosis. Thus, our data add a new layer to the oncogenic properties of S100A4 through its inhibition of p53-dependent processes.

Oncogene (2013) **32,** 5531–5540; doi:10.1038/onc.2013.213; published online 10 June 2013

Keywords: S100A4; p53; interaction study; proximity ligation assay; immunoprecipitation

INTRODUCTION

S100A4 (also known as MTS1 or FSP1) is a member of the S100 protein family comprising >20 members of small Ca^{2+}-binding proteins.[1,2] S100A4 has been intensively studied in human cancer and the data supporting its role in tumor progression is massive. Overexpression of S100A4 has been demonstrated in a wide range of cancer diseases for example, bladder,[3,4] endometrial,[5] pancreatic,[6,7] colorectal,[8–11] lung,[12,13] thyroid,[14] breast,[15–18] stomach[19] and prostate cancer.[20] In most cases the increased expression of S100A4 has been correlated with poor prognosis, and in many cases also with the development of metastasis.

The precise molecular function of S100A4 and other S100 proteins still remains to be described. S100 family members have no known enzymatic activity. Consequently, the biological functions of these proteins are generally believed to be through interaction with other proteins and regulation of these target protein functions. Several different S100A4-interacting proteins have been shown by various methods. The interaction between S100A4 and non-muscle myosin has so far been the focus of most investigations, and it has been suggested that S100A4 modulates the interaction between myosin and actin, which in turn affects rearrangement of the cytoskeleton.[21,22] Presumably, this is the reason for the connection between S100A4 and metastasis.[23–25] A direct interaction between p53 and S100A4 has also been shown by several groups using *in vitro* binding assays,[26–31] but the questions of the *in vivo* relevance and the functional consequence of this interaction has so far remained unresolved.[32]

We have previously shown that S100A4 is involved in the cellular response to ionizing radiation in a p53-dependent manner.[33] As irradiation elicits a multitude of cellular responses, our aim here was to investigate the direct role of S100A4 in response to p53 activation. For this purpose we treated cells with the p53-stabilizing agent Nutlin-3A,[34] and show that this treatment results in S100A4 stabilization. In addition, we show for the first time the interaction between endogenous S100A4 and p53 in cells using both immunoprecipitation (IP) and *in situ* proximity ligation assay (PLA), and that the interaction takes place within the cell nucleus. We also show that knockdown of S100A4 results in stabilization of p53 at the protein level. Further, knockdown of S100A4 is shown to increase the transcriptional activity of p53, resulting in p53-dependent growth arrest and increased cisplatin-induced apoptosis.

RESULTS

Increased p53 level results in stabilization of S100A4

Our previous research showed a p53-dependent S100A4 increase in response to ionizing radiation. To investigate whether p53 stabilization alone also affects the cellular S100A4 level, we treated A549 cells with Nutlin-3A. Nutlin-3A inhibits the interaction between p53 and MDM2, the ubiquitin E3 ligase mainly responsible for p53 ubiquitination, which targets p53 for proteasomal degradation. Treatment with 10 μM Nutlin-3A resulted in a rapid increase in p53 protein level, accompanied by an increase in the p53 transcriptional target p21 (Figure 1a). Supporting our previously published results we also detected an increase in S100A4. The increase in S100A4 was delayed compared with the increase in p21, indicating an alternative mechanism. Quantitative PCR analysis showed that the increase in p21 was through p53-dependent transcriptional upregulation as expected (Figure 1b). However, we could not detect any differences in the messenger RNA (mRNA) level of S100A4, indicating that the increase in S100A4 in response to Nutlin-3A was through stabilization of S100A4 at the protein level.

[1]Department of Oncology and Pathology, Karolinska Institutet, Science for Life Laboratory, Solna, Sweden; [2]Division of Toxicology, Institute of Environmental Medicine, Karolinska Institutet, Stockholm, Sweden and [3]Division of Molecular Biotechnology, School of Biotechnology, KTH, Royal Institute of Technology, AlbaNova University Center, Stockholm, Sweden. Correspondence: Dr LM Orre, Department of Oncology and Pathology, Karolinska Institutet, Science for Life laboratory, P O Box 1031, Solna, Stockholm 17121, Sweden. E-mail: lukas.orre@ki.se
Received 18 November 2012; revised 31 March 2013; accepted 3 May 2013; published online 10 June 2013

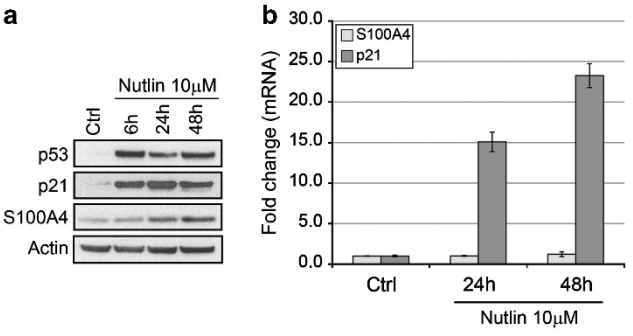

Figure 1. S100A4 is stabilized after Nutlin-3A treatment. (**a**) Immunoblot analysis of p53, p21 and S100A4 protein levels in A549 cells in response to Nutlin-3A treatment at indicated timepoints. (**b**) Quantitative real-time PCR analysis of S100A4 and p21 mRNA levels in A549 cells in response to Nutlin-3A treatment at indicated timepoints. Expression data is normalized to internal B2M RNA expression ($n = 3$; mean ± s.d.).

S100A4 interacts with p53 in the nucleus

S100 family proteins have no known enzymatic activity, and therefore it is generally believed that S100 proteins function through interaction with other proteins to regulate their functions. Previous reports have focused most attention to non-muscle myosin IIA and p53 as potential S100A4-interacting proteins. In the present studied system (A549 cells), fluorescence microscopy showed that S100A4 was mainly localized in the nucleus with no apparent myosin or f-actin (phalloidin) colocalization (Figure 2a). Nuclear colocalization between S100A4 and p53 was however apparent both in untreated and cisplatin-treated A549 cells (Supplementary Figure S1). Therefore, we decided to investigate the suggested interaction between S100A4 and p53. IP of endogenous S100A4 in A549 cells resulted in coprecipitation of endogenous p53 in untreated cells (Figure 2b). In addition, the amount of coprecipitated p53 increased after treatment of the cells with the p53-stabilizing drug Nutlin-3A (Figure 2b). To validate the interaction between S100A4 and p53 and to retrieve information about the subcellular location of the interaction, we performed *in situ* PLA[35] using antibodies targeting S100A4 and p53 (Figure 2c). The results from PLA supported the interaction between S100A4 and p53 in cells, and also underscored the dramatic increase in the interaction after treatment with Nutlin-3A. In addition, *in situ* PLA clearly showed that the subcellular location of the interaction between S100A4 and p53 was in the nucleus (Figure 2c and Supplementary Figure S2). Similar results were retrieved using another p53-stabilizing compound (the proteasome inhibitor MG132), another pair of antibodies directed against p53 and S100A4 and another p53 wild-type (wt) cell line (HeLa; Supplementary Figure S3).

Knockdown of S100A4 results in stabilization of p53 and transactivation of p53 transcriptional targets

As our data showed that S100A4 interacts with p53 in the nucleus, and that this interaction increased after inhibition of p53 degradation, we hypothesized that S100A4 could be involved in regulation of p53 degradation. We therefore constructed stable S100A4 small hairpin RNA (shRNA)-expressing A549 cells to investigate the impact of S100A4 on p53 stability. Western blotting showed efficient knockdown of S100A4 in S100A4 shRNA-expressing cells compared with cells transduced with the empty vector alone (Figure 3a). Interestingly, the protein levels of p53 and p21 were significantly increased in S100A4 shRNA-expressing cells. To validate these findings, we used small-interfering RNA (siRNA)-mediated knockdown of S100A4, targeting another part of the S100A4 mRNA. Transfections were performed in biological triplicates and the results fully supported the findings from shRNA-expressing cells as we detected efficient knockdown of S100A4 and increased p53 and p21 protein levels (Figure 3b). In addition, S100A4 siRNA resulted in increased level of MDM2, another p53 transcriptional target. In order to investigate the effects of S100A4 knockdown further, quantitative PCR analysis was performed after transfection of S100A4 siRNA. The mRNA level analysis showed that S100A4 siRNA efficiently knocked down S100A4 mRNA level, but we could not detect any change in p53 mRNA level, indicating that S100A4 knockdown stabilize p53 at the protein level (Figure 3c). The mRNA levels of p53 transcriptional targets p21 and MDM2 were increased after S100A4 knockdown, indicating increased p53 transcriptional activity. These effects of S100A4 knockdown were not exclusive to A549 cells, as we could see the same effects of siRNA-mediated S100A4 knockdown in HeLa cells, a cervical carcinoma cell line expressing wt p53 (Figure 3d). To validate that the increased p53 level in response to S100A4 knockdown that was due to increased p53 stability, we used cycloheximide treatment to block protein synthesis. Cycloheximide treatment of the cells indicated that p53 half-life was in fact increased in cells after S100A4 knockdown (Figure 3e and Supplementary Figure S4). Further supporting the impact of S100A4 on p53 stability, we could show that the difference in p53 protein level between S100A4 shRNA cells and control cells was greatly reduced after proteasome inhibition using MG132 (Figure 3f). As p53 stability is regulated by the ubiquitin E3 ligase MDM2, and a previous *in vitro* binding study showed a direct interaction between S100A4 and MDM2,[36] we used PLA assay to investigate the possible interaction between S100A4 and MDM2 in A549 cells after p53 stabilization using the proteasome inhibitor MG132. We could detect increased p53 and MDM2 interaction as well as increased S100A4 and MDM2 interaction in response to MG132 treatment (Supplementary Figure S5). We were however unable to detect mdm2 in S100A4 IP experiments as well as to detect S100A4 in MDM2 IP experiments (data not shown). These results were in concordance with the *in vitro* binding study[36] that also could not find evidence for a ternary complex between S100A4, p53 and MDM2. Taken together, these results indicate that S100A4 is involved in p53 degradation, and that loss of S100A4 results in increased p53 protein level and transcriptional activity.

S100A4 knockdown alone results in p53-dependent growth arrest but not apoptosis

As we could show that S100A4 knockdown resulted in stabilization of p53 and transcriptional activation of p53 target genes, we investigated the effect of S100A4 knockdown on cellular processes known to be regulated by p53. Performing short-term cell viability assays, we could show that siRNA-mediated knockdown of S100A4 in both A549 cells and HeLa cells resulted in a reduced number of viable cells (Figure 4a). Measurements of the relative growth in S100A4 shRNA cells and empty vector cells supported these findings (Supplementary Figure S6). The effect of S100A4 knockdown on cell viability was greatly reduced when combined with p53 siRNA, indicating that the effect of S100A4 knockdown on cell viability was p53 dependent (Figure 4b). Cell cycle analysis by flow cytometry showed that knockdown of S100A4 resulted in a p53-dependent G1 arrest, but no increase in the sub-G1 population, indicating that there was no increase in apoptosis by S100A4 knockdown alone (Figures 4c and d). These findings were supported by the lack of poly (ADP-ribose) polymerase cleavage in response to S100A4 knockdown (Figure 4e). In addition, we could show that the increase in p21 level detected in response to S100A4 knockdown was abolished when p53 was knocked down at the same time (Figure 4f). The results thus indicate that the increase in p53 induced by S100A4

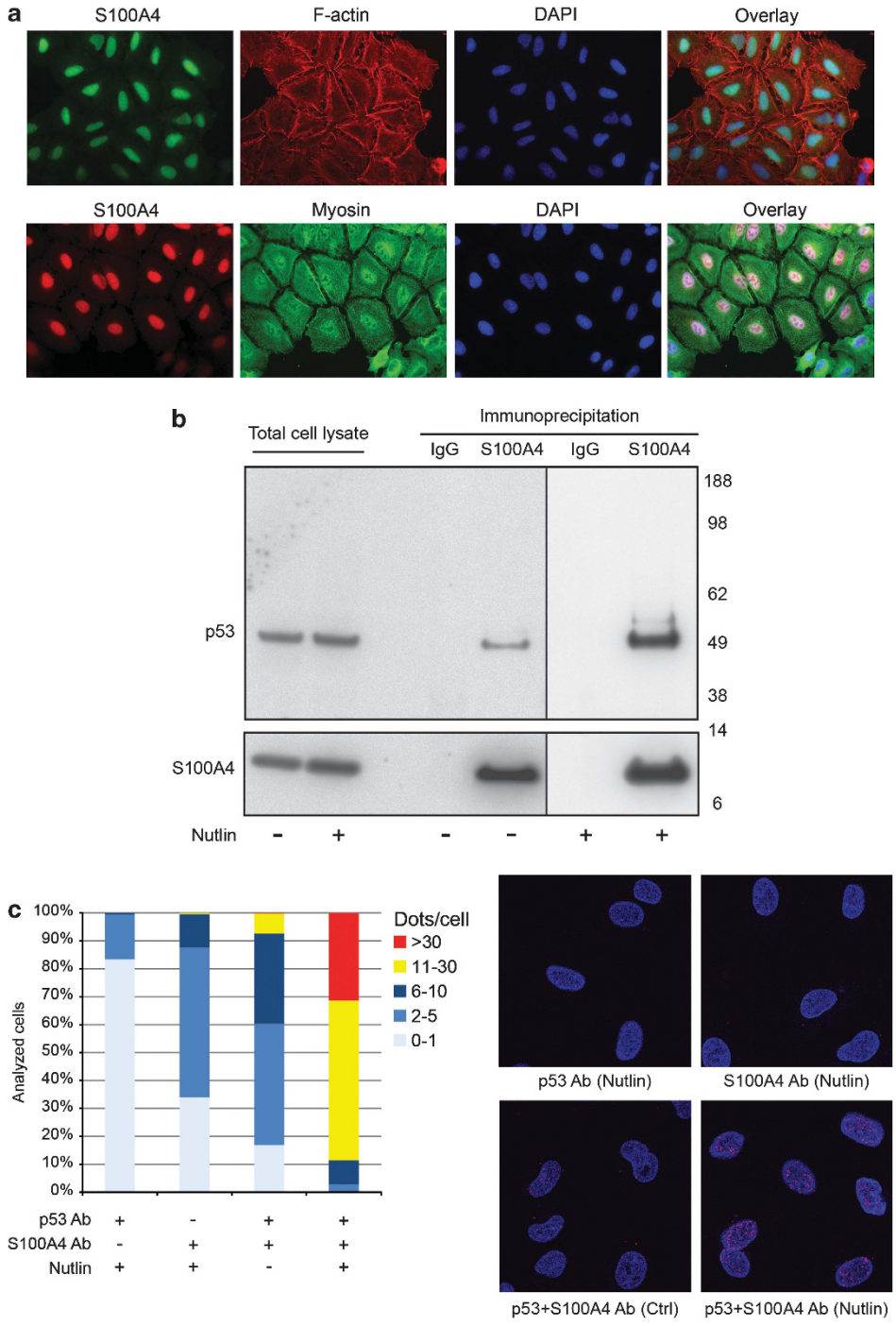

Figure 2. S100A4 interacts with p53 in the nucleus. (**a**) Fluorescence microscopy images of S100A4 subcellular location in untreated A549 cells in relation to f-actin staining (phalloidin) and non-muscle myosin IIA staining. (**b**) Immunoblot analysis of p53 and S100A4 protein in S100A4 IP experiments in untreated and Nutlin-3A-treated (10μM) A549 cells. (**c**) *In situ* PLA of S100A4–p53 interaction in A549 cells +/− Nutlin-3A. As a negative control, either S100A4 or p53 antibody was excluded from the assay. Data represents the number of interaction signals (dots) per cell from three independent experiments ($n = 100$ cells per condition/experiment). Representative images from PLA for each condition is shown on the right. Nuclei are defined by Hoechst staining.

knockdown, leads to p53-dependent cell cycle arrest, but not apoptosis.

Knockdown of S100A4 results in increased cisplatin-induced apoptosis

S100A4 knockdown by itself did not induce apoptosis, but still the increased p53 levels could prime the cells for apoptosis activation. To investigate whether this was the case, we used cisplatin, a cytotoxic drug that induces apoptosis in a p53-dependent manner. Using both short-term cell viability assay and clonogenic survival assay, we detected increased cisplatin sensitivity in S100A4 shRNA cells compared with control cells (Figure 5 and Supplementary Figure S7). To further study the cisplatin response during S100A4 knockdown, we used several assays to evaluate cell death. Silencing of S100A4 significantly

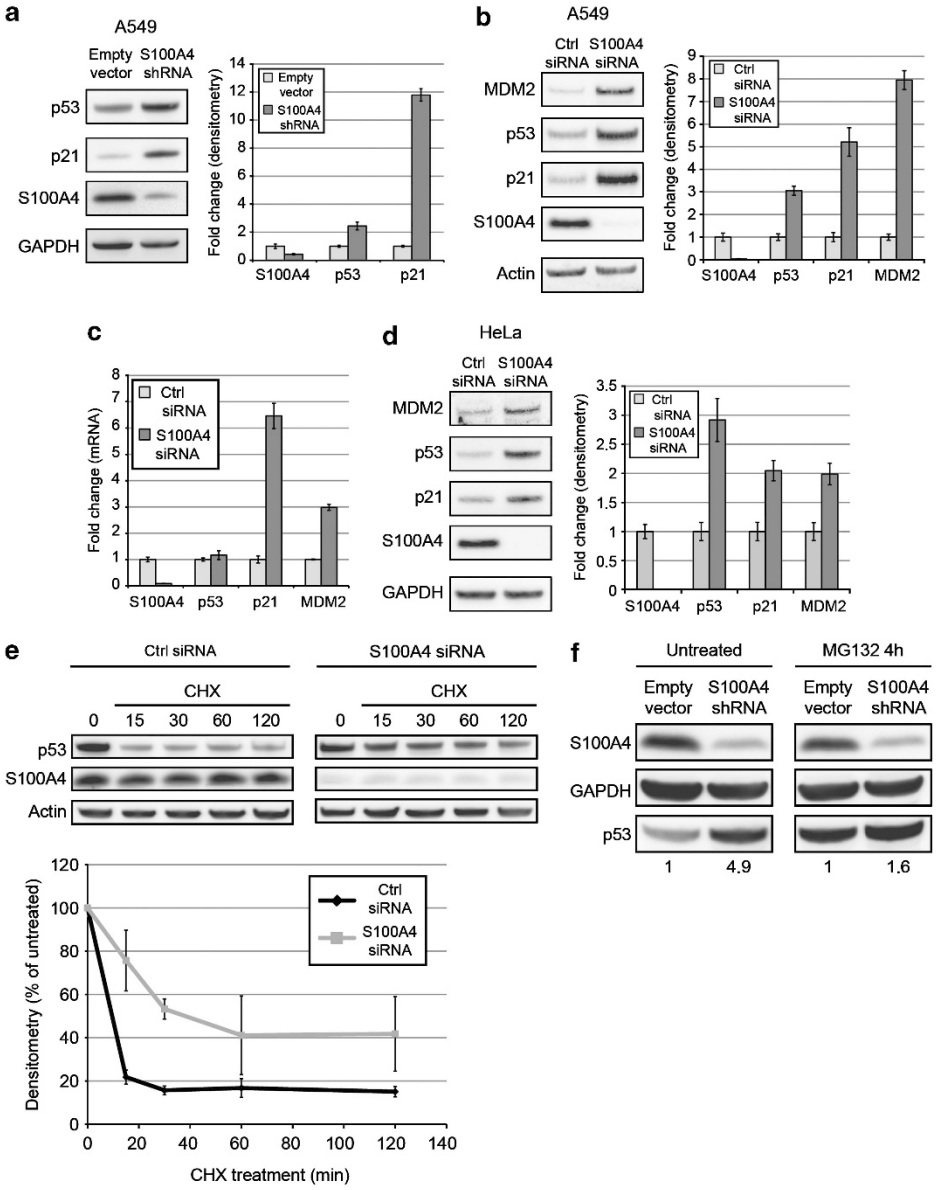

Figure 3. Knockdown of S100A4 results in p53 stabilization. (**a**) Immunoblot analysis of S100A4, p53 and p21 in A549 cells stably expressing S100A4 shRNA. Densitometric analysis showing fold change in protein levels compared with empty vector cells is also shown ($n = 3$; mean ± s.d.). (**b**) Immunoblot analysis of S100A4, p53, p21 and MDM2 in A549 cells 72 h after transfection with S100A4 siRNA. Densitometric analysis showing fold change in protein levels compared with cells transfected with control siRNA is also shown ($n = 3$; mean ± s.d.). (**c**) Quantitative real-time PCR analysis of S100A4, p53, p21 and MDM2 mRNA levels in A549 cells transfected with S100A4 siRNA. Expression data were normalized to internal 18S ribosomal RNA expression and presented as fold change compared with cells transfected with control siRNA ($n = 3$; mean ± s.d.). (**d**) Immunoblot analysis of S100A4, p53, p21 and MDM2 in HeLa cells transfected with S100A4 siRNA. Densitometric analysis showing fold change in protein levels compared with cells transfected with control siRNA is also shown ($n = 3$; mean ± s.d.). (**e**) Immunoblot analysis showing p53 and S100A4 protein levels in A549 cells (+/− S100A4 siRNA) treated with cycloheximide (25 μg/ml) at indicated timepoints. Densitometric analysis is also shown ($n = 3$; mean ± s.d.). (**f**) Immunoblot analysis of p53 and S100A4 protein levels in A549 shRNA cells and empty vector cells after treatment with MG132 (10 μM, 4 h). Relative density of p53 bands normalized to glyceraldehyde 3-phosphate dehydrogenase (GAPDH) is indicated below the blot.

increased caspase-3-like activity and accumulation of its specific cleavage product poly (ADP-ribose) polymerase-1, markers of apoptotic cell death (Figures 6a and b). Furthermore, knockdown of S100A4 resulted in increased cisplatin-induced apoptosis measured by Annexin V-binding assay that was also accompanied by a drop in mitochondrial membrane potential (Figures 6c and d). To validate that the increase in cisplatin-dependent apoptosis was due to p53 stabilization, we measured apoptosis also in cells where p53 was knocked down using transfection with p53 siRNA. In this rescue experiment, knockdown of p53 efficiently inhibited cisplatin-induced apoptosis and eliminated the difference between S100A4 shRNA-expressing cells and empty vector cells (Figure 6e). All apoptosis assays showed no significant difference in apoptosis between untreated empty vector cells and untreated S100A4 shRNA cells. Taken together, our data show that knockdown of S100A4

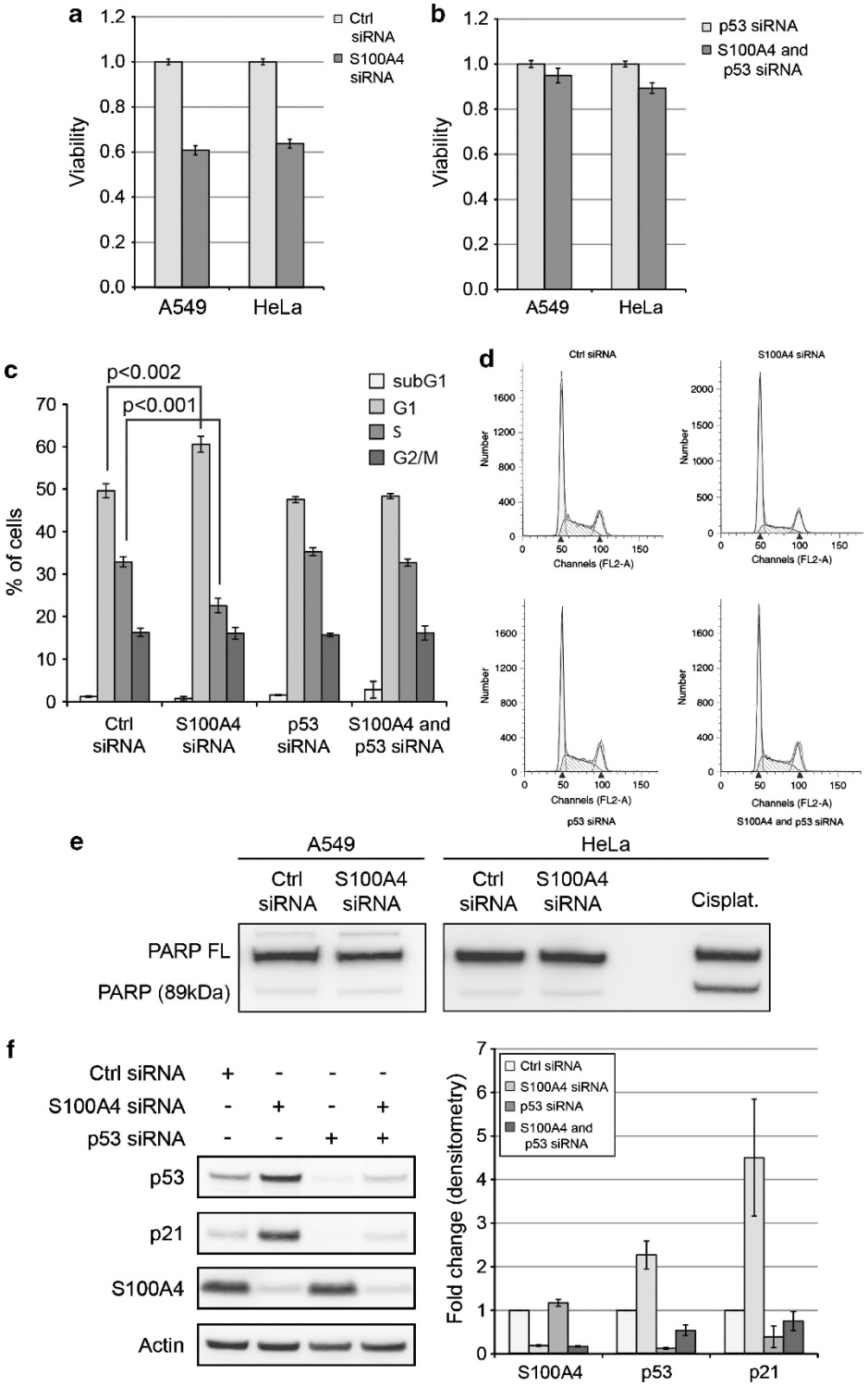

Figure 4. Knockdown of S100A4 results in growth arrest. (**a**) Cell viability assay in A549 and HeLa cells transfected with S100A4 siRNA or control siRNA. Viability was measured 72 h after transfection with siRNA ($n = 3$; mean ± s.d.). (**b**) Cell viability assay in A549 and HeLa cells transfected with p53 siRNA alone or in combination with S100A4 siRNA. Viability was measured 72 h after transfection with siRNA ($n = 3$; mean ± s.d.). (**c**) Cell cycle analysis in A549 cells transfected with S100A4 siRNA and p53 siRNA alone or in combination ($n = 3$; mean ± s.d.). (**d**) Representative images from cell cycle analysis performed with ModFit software (Verity Software House, Topsham, ME, USA). (**e**) Immunoblot analysis of poly (ADP-ribose) polymerase (PARP) cleavage in response to S100A4 siRNA in A549 and HeLa cells. PARP cleavage in response to cisplatin (1.5 μg/ml) in HeLa cells is shown as reference. (**f**) Immunoblot analysis of S100A4, p53 and p21 in A549 cells transfected with S100A4 siRNA and p53 siRNA alone or in combination. Densitometric analysis showing fold change in protein levels compared with cells transfected with control siRNA is also shown ($n = 3$; mean ± s.d.).

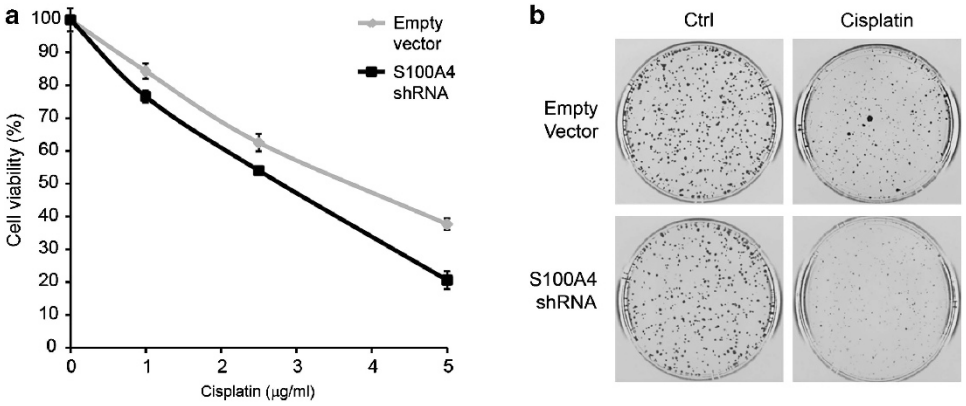

Figure 5. Knockdown of S100A4 results in increased cisplatin sensitivity. (**a**) Cell viability assay in A549 S100A4 shRNA cells and empty vector cells treated with different concentrations of cisplatin for 72 h ($n = 3$; mean ± s.d.). (**b**) Clonogenic assay in A549 S100A4 shRNA cells and empty vector cells treated with 0.5 μg/ml cisplatin for 24 h.

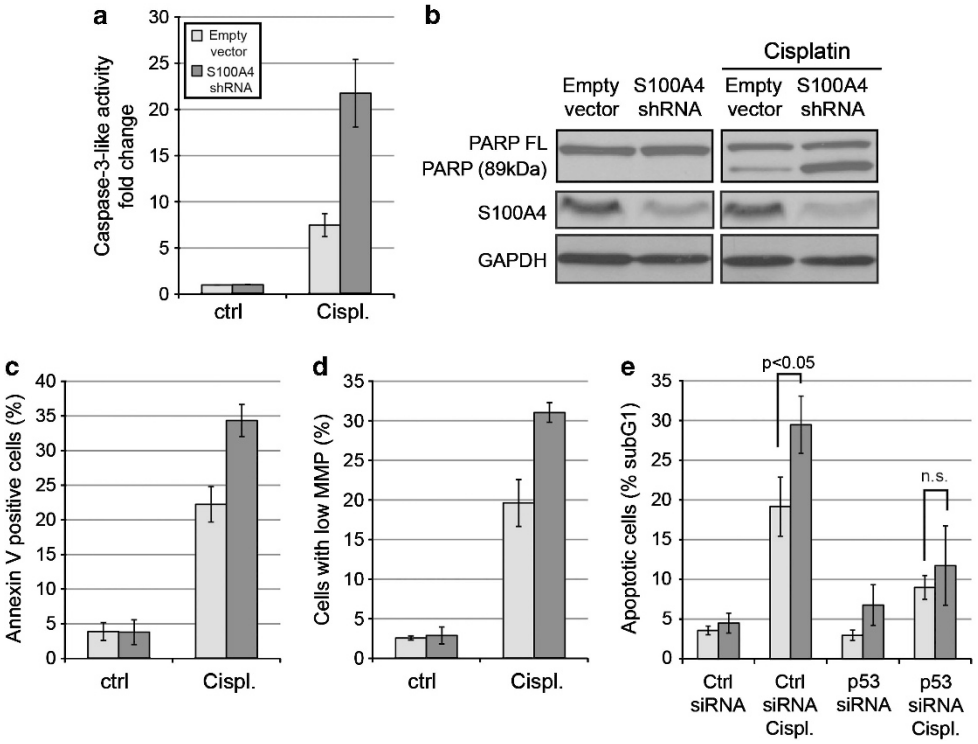

Figure 6. Knockdown of S100A4 results in increased cisplatin-induced apoptosis. (**a**) The effect of S100A4 shRNA on caspase-3-like activity in A549 cells treated with cisplatin (48 h, 5 μg/ml). (**b**) Immunoblot analysis of PARP and S100A4 protein levels after treatment with cisplatin (48 h, 5 μg/ml) in A549 shRNA cells and empty vector cells. (**c**) The effect of S100A4 shRNA on Annexin V staining in A549 cells treated with cisplatin (48 h, 5 μg/ml). (**d**) The effect of S100A4 shRNA on mitochondrial membrane potential (MMP) in A549 cells treated with cisplatin (48 h, 5 μg/ml). MMP was assessed by tetramethylrhodamine ethyl ester staining. (**e**) The effect of p53 knockdown by siRNA on apoptosis estimated by sub-G1 cells in A549 shRNA and empty vector cells after treatment with cisplatin (48 h, 5 μg/ml). Where applicable, ($n = 3$; mean ± s.d.).

results in increased p53-dependent apoptosis in response to cisplatin treatment.

DISCUSSION

In this study, we report on the interaction between S100A4 and p53 in the nucleus, and also that S100A4 negatively affects cellular p53 protein levels. *In vitro* binding studies by several different groups have shown a direct interaction between recombinant p53 and S100A4 using different methods,[26–31] but so far in cell data has been missing.[32] The only previously published report of interaction between S100A4 and p53 in a complex sample involved co-IP from cells harboring mutant p53.[28] The reason for the difficulty in detecting the interaction in cells could be that the complex is short lived or dependent on high local concentration of the interactors or the intactness of subcellular compartments.[37] In order to circumvent these difficulties, we added an additional step, *in vivo* crosslinking, to the IP protocol. It has previously been shown that *in vivo* crosslinking can increase the sensitivity of the assay and increase the possibility of detecting relevant

interactions.[38] In addition, to validate the findings from co-IP experiments, we used *in situ* PLA to investigate the interaction between p53 and S100A4. Using this approach not only could we confirm the interaction between S100A4 and wt p53, but also that this interaction takes place in the cell nucleus.

Another type of interactions that are typically difficult to detect are those between ubiquitin ligases and their substrates, as these interactions are transient and results in rapid degradation of the ubiquitinated substrate.[39] Intriguingly, we show here that the interaction between S100A4 and p53 is dramatically increased after disruption of the interaction between p53 and its ubiquitin ligase MDM2 using Nutlin-3A. In untreated cells, however, the interaction between p53 and MDM2 results in rapid MDM2-dependent p53 ubiquitination and degradation. If the interaction between S100A4 and p53 is a step in the cellular processes resulting in p53 ubiquitination and degradation, this could explain the difficulty in detecting the interaction between p53 and S100A4. Together with the nuclear localization of the interaction between S100A4 and p53, and the fact that reduced S100A4 levels results in increased p53 stability, our data suggests that S100A4 is involved in MDM2-dependent p53 ubiquitination and degradation. This hypothesis is also supported by a recent report showing that S100A4 destabilize wt p53 in co-transfection experiments in H1299 (p53-null) cells.[40] Another study using colon cancer cell line HCT116 could however not find any evidence of mutual regulation between S100A4 and p53, suggesting differences between cell types.[41]

MDM2-dependent p53 ubiquitination has been shown to be affected by p53 acetylation,[42] but also by p53 oligomerization[43] and p53 phosphorylation.[44,45] *In vitro* studies of the interaction between S100A4 and p53 has shown that S100A4 binds to the C-terminal part of p53[28] containing multiple lysine residues that can be either acetylated (protects p53 from degradation) or ubiquitinated (tags p53 for degradation). Through this binding, S100A4 could potentially affect the balance of p53 modifications in the negative regulatory domain, resulting in increased p53–MDM2 affinity and increased p53 ubiquitination. Other studies have suggested higher affinity of S100A4 to the nuclear export signal domain and the tetramerization domain of p53, and that S100A4 regulates p53 oligomerization.[27] Later on it was shown that this effect of S100A4 was not unique to p53, but that also the oligomerization state of p63 and p73 was regulated by S100A4.[46] It has been shown that the p53 oligomerization state also affects its acetylation and stability,[43,47] providing an additional explanation to the findings reported here. Interestingly, an *in vitro* interaction between S100A4 and the N-terminal domain of MDM2 (residues 2–125) was recently shown,[36] presenting yet another mechanism through which S100A4 could increase p53 degradation. The interaction between p53 and MDM2 has been shown to be dependent on multiple regions on both p53 and MDM2. Of particular interest in this context is the interaction between the N-terminal part of MDM2 (residues 10–139) and the C-terminal part of p53 (residues 367–397)[48] as S100A4 has been shown to interact with these regions of p53 and MDM2. In the present study, we did find evidence for an interaction between S100A4 and MDM2, but we were unable to show evidence for a ternary complex between S100A4, p53 and MDM2, which was also not detected in the previously published *in vitro* study.[36] Although it is possible that the formation of a ternary complex between p53, MDM2 and S100A4 increases the degradation rate of p53, our data suggest that S100A4 and MDM2 act in sequence to promote p53 degradation.

The findings presented here are of specific importance as p53 is one of the most well-established tumor suppressor proteins known. An overwhelming amount of data suggest that p53 inactivation is virtually necessary for tumor development and progression. Without p53 inactivation oncogenic cells would inevitably undergo rapid cell cycle arrest and/or apoptosis. In roughly half of all tumors, p53 is mutated, which abolishes or greatly inhibits its normal cellular functions. In the remaining tumors, the activities of p53 are most likely inhibited by other means such as inactivation of downstream signaling or increased p53 degradation. Several different mechanisms for increased p53 degradation in tumors have so far been described. In some cases, tumor cells have an increased expression of ubiquitin E3-ligases such as MDM2, COP1 and PIRH2 (RCHY1), all promoting proteasomal p53 degradation.[49] These ligases are normally involved in negative feedback regulation, as they are transcriptional targets of p53, ensuring that the cellular level of p53 is kept low in normal cells. Another mechanism of increased p53 degradation in tumors is through the loss of p14ARF expression. p14ARF is an inhibitor of MDM2, and loss of p14ARF results in the loss of MDM2 inhibition and increased p53 degradation.[50] Our data suggest that S100A4, a protein that is widely overexpressed in tumors and in many cases correlated with poor prognosis, through its interaction with p53 contributes to p53 degradation. Very few clinical studies have been performed where the expression level of p53 and S100A4 is determined in the same material; however, a strong inverse correlation between S100A4 and p53 has been shown by immunohistochemistry in lung adenocarcinoma, suggesting that the level of S100A4 is higher in p53 wt tumors.[13] We have previously reported expression of S100A4 and p53 in stage I non-small cell lung cancer but without finding a significant correlation, although 18 of 22 S100A4-positive tumors showed negative p53 staining (indicating that p53 is wt).[51] A trend toward inverse correlation between S100A4 and p53 was also shown in a breast cancer cohort, where a higher level of S100A4 was found to be a negative prognostic factor.[18] To fully appreciate the impact of S100A4 on p53 in cancer, directed analysis considering also p53 mutational status and the expression of p53 ubiquitin ligases and other factors affecting p53 degradation will be needed.

In addition to our results describing the interaction between p53 and S100A4 and the negative impact of S100A4 expression on p53 protein level, we have also shown that knockdown of S100A4 results in p53-dependent cell cycle arrest and increased cisplatin-dependent apoptosis. These findings clearly demonstrate why high S100A4 expression would be beneficial for tumor growth, providing an explanation for the negative prognostic impact of S100A4 shown in clinical studies. Taken together, our data presented here suggest that in addition to increasing the risk of metastasis as previously shown, a high expression of S100A4 in tumors has the potential of inhibiting the activities of p53. This data also suggest that S100A4 expression should be studied in clinical samples in relation to cisplatin sensitivity to investigate the potential use of S100A4 as a predictive marker for cisplatin therapy response.

MATERIALS AND METHODS

Antibodies and reagents

The following antibodies were used: p53 DO-1 (sc-126), p21 C-19 (sc-397), Actin I-19 (sc-1616) and MDM2 SMP14 (sc-965) from Santa Cruz Biotechnology (Santa Cruz, CA, USA); S100A4 (A5114) from Dako (Ely, UK); S100A4-3 (CPTC) from DSHB (Iowa, IA, USA); GAPDH (G8795), from Sigma-Aldrich (Gillingham, UK); p53 (#2527), poly (ADP-ribose) polymerase (#9542) and cleaved poly (ADP-ribose) polymerase 19F4 (#9546) from Cell Signaling Technology (Danvers, MA, USA); GAPDH (2275-PC-100) from Trevigen (Gaithersburg, MD, USA) and non-muscle myosin IIA (ab24762) from Abcam (Cambridge, MA, USA). The following reagents were used: Nutlin-3A (N6287), cycloheximide (C4859), MG132 (C2211) and cisplatin (P4394) from Sigma-Aldrich.

Cell lines and cell cultures

The lung cancer cell line A549, as well as A549 (S100A4 shRNA) and A549 (empty vector) cell lines were cultured in Roswell Park Memorial Institute medium-1640 with 10% calf serum and 100 μg/ml penicillin/streptomycin (Invitrogen, Life Technologies, Carlsbad, CA, USA). HeLa cells were cultured

in Dulbecco's modified Eagle's medium with 10% calf serum and 100 μg/ml penicillin/streptomycin (Invitrogen, Life Technologies). A549 and HeLa cells were from ATCC (Manassas, VA, USA).

For the generation of stable S100A4 shRNA-expressing cells, the pLKO.1 plasmid expressing shRNA for S100A4 (target sequence 5′-GCUCAACAA GUCAGAACUAAA-3′, RHS3979-9620807) and the control pLKO.1 plasmid (empty vector, RHS4080) were obtained from Open Biosystems (Thermo Fisher Scientific, Waltham, MA, USA). The helper plasmids for viral vector production, pG32231 and pMD2.G, were a kind gift from Professor Didier Trono at the School of Life Sciences, EPFL, Lausanne, Switzerland. HEK-293T cells (LGC Promochem, Boras, Sweden) were transfected with plasmids for virus production by the calcium-phosphate method. In brief, plasmids were mixed with 124 mM $CaCl_2$ in HEPES (4-(2-hydroxyethyl)-1-piperazineethanesulfonic acid)-buffered saline (140 mM NaCl, 50mM HEPES, 1 mM Na_2HPO_4, pH 7.1) and added to 40% confluent HEK-293T cells in Iscove's modified Dulbecco's medium supplemented with 10% fetal bovine serum. After 16 h, medium was replaced with DMEM supplemented with 10% fetal bovine serum, 10 mM HEPES, 1% non-essential amino acids and 1% penicillin/streptomycin, all from Invitrogen, Life Technologies. Viral supernatants were harvested 50 h after transfection and added to A549 cells. Transduced A549 cells were subsequently selected using 1 μg/ml puromycin (Sigma-Aldrich) in the culture medium, after which resistant clones were expanded and tested for efficient S100A4 knockdown using western blot.

Immunofluorescence

For fluorescence microscopy, A549 cells grown on cover slides were washed in phosphate-buffered saline (PBS) and fixed in 4% formaldehyde/PBS. Cells were then washed in PBS, permeabilized using 0.1% Triton X-100/PBS, washed again and blocked in 5% bovine serum albumin/PBS. After incubation with primary antibodies against S100A4 (mouse, DSHB) or S100A4 and myosin (rabbit, Abcam, in 5% bovine serum albumin/PBS) overnight at 4 °C, the cells were washed and incubated with fluorophore-conjugated secondary antibodies (Alexa-488 goat anti-mouse IgG (A11001), Alexa-568 goat anti-mouse IgG (A1104) or Alexa-488 goat anti-rabbit IgG (A11008)) and/or phalloidin (Alexa-568 labeled, A12380). The cells were then washed in PBS, followed by staining of nuclei (DNA) using DAPI (D3571) and mounted on microscope slides using Prolong Gold (P36934). Reagents were obtained from Invitrogen, Life Technologies. Fluorescence images were obtained using a Leica DMRXA fluorescence microscope (Leica, Wetzlar, Germany).

siRNA transfection

For S100A4 knockdown ON-TARGETplus siRNA (J-004792-08) was used with the target sequence 5′-GUGACAAGUUCAAGCUCAA-3′, and for p53 knockdown ON-TARGETplus SMARTpool (L-003329-00) was used (Dharmacon, Thermo Fisher Scientific, Waltham, MA, USA). As siCtrl, ON-TARGETplus Non-targeting siRNA (D-001810-01) was used in all experiments. Transfection of siRNA was performed using Lipofectamine RNAiMAX (Invitrogen, Life Technologies), following the standard protocol for reverse transfection.

Quantitative PCR analysis

mRNA was extracted using the RNeasy Mini Kit (Qiagen, Hilden, Germany) and the concentration was measured using a NanoDrop (Thermo Fisher Scientific). Fifty nanograms of RNA was retrotranscribed using High Capacity RNA-to-cDNA kit (Invitrogen, Life Technologies), according to manufacturer's recommendations. Ten nanograms of complementary DNA was used for each quantitative PCR reaction and the reactions were performed in a 96-well plates using TaqMan Gene Expression Assay (Invitrogen, Life Technologies). The following assays were used: S100A4 (Hs00243202_m1), p21 (Hs00355782_m1), MDM2 (Hs00242813_m1) and p53 (Hs01034249_m1). For normalization purposes either B2M (Hs99999907_m1) or 18S (Hs99999901_s1) was used. Changes in mRNA levels were expressed as fold change, which was calculated with the $\Delta\Delta C_t$ method based on C_t cycle values for the target gene of interest normalized to B2M or 18S.

Proximity ligation assay

For PLA, cells were seeded on cover slides and treated with either Nutlin-3A (72 h) or MG132(4 h). The slides were then treated as described for immunofluorescence up to the point of overnight incubation with primary antibodies. The following antibody pairs were used in combination or alone as negative controls: p53 (DO-1, mouse)/S100A4 (A5114, rabbit); p53 (#2527, rabbit)/S100A4 (CPTC, mouse); S100A4 (A5114, rabbit)/MDM2 (SMP14, mouse) and p53 (#2527, rabbit)/MDM2 (SMP14, mouse). After washing, the slides were treated according to manufacturer's protocol using the Duolink Detection Kit with PLA PLUS and MINUS Probes for mouse and rabbit (Olink Bioscience, Uppsala, Sweden). Hoechst stain was included in the Duolink Detection Kit. Specimens were examined with a Zeiss LSM 780 confocal microscope (Zeiss, Oberkochen, Germany) under a 63 × /oil objective for fluorescent Texas Red and blue DAPI signals. The number of *in situ* PLA signals per cell was counted by image analysis with the CellProfiler software (http://www.cellprofiler.org). Nuclei edges were delineated based on the Hoechst staining. Analysis parameters were defined and used consistently throughout all experiments. The signals were counted in at least 100 cells per replicate, in biological triplicates.

Covalent coupling of antibodies to beads

For each IP reaction, antibodies (5 μg) were covalently coupled to 20 μl of Protein A/G PLUS-Agarose (Santa Cruz Biotechnology), using dimethyl pimelimidate dihydrochloride (Sigma-Aldrich), as previously described.[51] The antibody-coupled beads were washed with the IP buffer (50 mM Tris-HCl pH 7.5, 150 mM NaCl, $CaCl_2$ 2 mM and Halt Protease and Phosphatase Inhibitor Cocktail, EDTA-Free, Thermo Fisher Scientific) and used the same day for IP.

In vivo crosslinking of protein complexes and IP

A549 cells were harvested, washed with PBS and incubated 20 min at 37 °C in 0.125% paraformaldehyde/PBS. To stop the crosslinking reaction, 125 mM glycine was added for 5 min at room temperature. Cells were then washed twice with PBS, and resuspended in lysis buffer (150 mM NaCl, 50 mM Tris-HCl pH 7.5, 1% Triton X-100, 1% CHAPS, 10% glycerol, 0.05% SDS, 2 mM $CaCl_2$) containing protease/phosphatase inhibitors. Cell lysates were centrifuged for 10 min at 12 000 r.p.m. to pellet cell debris. Supernatants were collected and protein levels quantified using DC-protein assay (Bio-Rad Laboratories, Hercules, CA, USA).

For each IP reaction, total protein lysate (1 mg) was diluted to 1 ml in IP buffer. Samples were precleared with 20 μl Protein A/G PLUS-Agarose (Santa Cruz Biotechnology) in IP buffer (25% slurry) for 1 h at 4 °C. Precleared lysates were then incubated with the prepared antibody-coupled beads overnight at 4 °C. After washing in IP buffer, captured proteins were eluted and crosslinking reverted by incubating for 30 min at 95 °C with 20 μl NuPAGE LDS Sample Buffer (Invitrogen, Life Technologies).

Western blotting

Proteins were separated on NuPAGE Bis-Tris gels using Novex gel electrophoresis system (Invitrogen, Life Technologies) and transferred onto Amersham Hybond C Extra nitrocellulose membranes (GE Healthcare, Waukesha, WI, USA). Membranes were then blocked with 5% milk (Bio-Rad Laboratories), incubated with primary antibody overnight at 4 °C, washed in 0.1% Tween-20/Tris-buffered saline, and incubated with secondary antibody (anti-mouse (NA931V) or anti-rabbit (NA934V) from GE Healthcare for 1 h at room temperature. After washing, membranes were incubated in Amersham ECL prime reagent, and visualization and densitometric analysis was performed using ImageQuant LAS 4000 and ImageQuant TL image analysis software (GE Healthcare). Relative protein quantifications were done after normalization against appropriate loading controls.

Cell viability assays

For estimation of cell viability in response to S100A4 and p53 siRNA in A549 and HeLa cells, respectively, CellTiter-Blue assay (Promega, Madison, WI, USA) was used according to the manufacture's protocol. For estimation of cell viability in response to cisplatin in A549 S100A4 shRNA and empty vector cells, CellTiter 96 AQueous Non-Radioactive Cell Proliferation Assay (Promega) was performed according to the manufacture's protocol. Results presented are the means ± s.d. of three independent experiments.

Cell cycle analysis, clonogenic assay and apoptosis assays

Cell cycle analysis, clonogenic assay and apoptosis assays including caspase activity assay, Annexin V/PI staining and mitochondrial membrane potential were performed, as published previously.[52]

CONFLICT OF INTEREST

The authors declare no conflict of interest.

ACKNOWLEDGEMENTS

We thank Professor Didier Trono at the School of Life Sciences, EPFL, Lausanne, Switzerland for providing the helper plasmids for viral vector production, pG32231 and pMD2.G. We also thank the group of Professor Hjalmar Brismar for assistance in the use of confocal microscopy. This study was supported by grants from the Swedish and Stockholm Cancer Societies, the Swedish Research Foundation, the Swedish Research council, the Swedish Childhood Cancer Society, the European Union (Chemores and Apo-Sys). VOK was supported by a fellowship from the Swedish Institute and Karolinska Institutet. EP was supported by Karolinska Institutet KID funding.

REFERENCES

1 Heizmann CW. The multifunctional S100 protein family. *Methods Mol Biol* 2002; **172**: 69–80.
2 Santamaria-Kisiel L, Rintala-Dempsey AC, Shaw GS. Calcium-dependent and -independent interactions of the S100 protein family. *Biochem J* 2006; **396**: 201–214.
3 Davies BR, O'Donnell M, Durkan GC, Rudland PS, Barraclough R, Neal DE *et al.* Expression of S100A4 protein is associated with metastasis and reduced survival in human bladder cancer. *J Pathol* 2002; **196**: 292–299.
4 Matsumoto K, Irie A, Satoh T, Ishii J, Iwabuchi K, Iwamura M *et al.* Expression of S100A2 and S100A4 predicts for disease progression and patient survival in bladder cancer. *Urology* 2007; **70**: 602–607.
5 Xie R, Loose DS, Shipley GL, Xie S, Bassett Jr RL, Broaddus RR. Hypomethylation-induced expression of S100A4 in endometrial carcinoma. *Mod Pathol* 2007; **20**: 1045–1054.
6 Oida Y, Yamazaki H, Tobita K, Mukai M, Ohtani Y, Miyazaki N *et al.* Increased S100A4 expression combined with decreased E-cadherin expression predicts a poor outcome of patients with pancreatic cancer. *Oncol Rep* 2006; **16**: 457–463.
7 Rosty C, Ueki T, Argani P, Jansen M, Yeo CJ, Cameron JL *et al.* Overexpression of S100A4 in pancreatic ductal adenocarcinomas is associated with poor differentiation and DNA hypomethylation. *Am J Pathol* 2002; **160**: 45–50.
8 Cho YG, Kim CJ, Nam SW, Yoon SH, Lee SH, Yoo NJ *et al.* Overexpression of S100A4 is closely associated with progression of colorectal cancer. *World J Gastroenterol* 2005; **11**: 4852–4856.
9 Flatmark K, Pedersen KB, Nesland JM, Rasmussen H, Aamodt G, Mikalsen SO *et al.* Nuclear localization of the metastasis-related protein S100A4 correlates with tumour stage in colorectal cancer. *J Pathol* 2003; **200**: 589–595.
10 Gongoll S, Peters G, Mengel M, Piso P, Klempnauer J, Kreipe H *et al.* Prognostic significance of calcium-binding protein S100A4 in colorectal cancer. *Gastroenterology* 2002; **123**: 1478–1484.
11 Hemandas AK, Salto-Tellez M, Maricar SH, Leong AF, Leow CK. Metastasis-associated protein S100A4--a potential prognostic marker for colorectal cancer. *J Surg Oncol* 2006; **93**: 498–503.
12 Kimura K, Endo Y, Yonemura Y, Heizmann CW, Schafer BW, Watanabe Y *et al.* Clinical significance of S100A4 and E-cadherin-related adhesion molecules in non-small cell lung cancer. *Int J Oncol* 2000; **16**: 1125–1131.
13 Matsubara D, Niki T, Ishikawa S, Goto A, Ohara E, Yokomizo T *et al.* Differential expression of S100A2 and S100A4 in lung adenocarcinomas: clinicopathological significance, relationship to p53 and identification of their target genes. *Cancer Sci* 2005; **96**: 844–857.
14 Zou M, Al-Baradie RS, Al-Hindi H, Farid NR, Shi Y. S100A4 (Mts1) gene overexpression is associated with invasion and metastasis of papillary thyroid carcinoma. *Br J Cancer* 2005; **93**: 1277–1284.
15 Lee WY, Su WC, Lin PW, Guo HR, Chang TW, Chen HH. Expression of S100A4 and Met: potential predictors for metastasis and survival in early-stage breast cancer. *Oncology* 2004; **66**: 429–438.
16 Pedersen KB, Nesland JM, Fodstad O, Maelandsmo GM. Expression of S100A4, E-cadherin, alpha- and beta-catenin in breast cancer biopsies. *Br J Cancer* 2002; **87**: 1281–1286.
17 Platt-Higgins AM, Renshaw CA, West CR, Winstanley JH, De Silva Rudland S, Barraclough R *et al.* Comparison of the metastasis-inducing protein S100A4 (p9ka) with other prognostic markers in human breast cancer. *Int J Cancer* 2000; **89**: 198–208.
18 Rudland PS, Platt-Higgins A, Renshaw C, West CR, Winstanley JH, Robertson L *et al.* Prognostic significance of the metastasis-inducing protein S100A4 (p9Ka) in human breast cancer. *Cancer Res* 2000; **60**: 1595–1603.
19 Cho YG, Nam SW, Kim TY, Kim YS, Kim CJ, Park JY *et al.* Overexpression of S100A4 is closely related to the aggressiveness of gastric cancer. *Apmis* 2003; **111**: 539–545.
20 Gupta S, Hussain T, MacLennan GT, Fu P, Patel J, Mukhtar H. Differential expression of S100A2 and S100A4 during progression of human prostate adenocarcinoma. *J Clin Oncol* 2003; **21**: 106–112.
21 Kriajevska M, Bronstein IB, Scott DJ, Tarabykina S, Fischer-Larsen M, Issinger O *et al.* Metastasis-associated protein Mts1 (S100A4) inhibits CK2-mediated phosphorylation and self-assembly of the heavy chain of nonmuscle myosin. *Biochim Biophys Acta* 2000; **1498**: 252–263.
22 Li ZH, Bresnick AR. The S100A4 metastasis factor regulates cellular motility via a direct interaction with myosin-IIA. *Cancer Res* 2006; **66**: 5173–5180.
23 Ambartsumian NS, Grigorian MS, Larsen IF, Karlstrom O, Sidenius N, Rygaard J *et al.* Metastasis of mammary carcinomas in GRS/A hybrid mice transgenic for the mts1 gene. *Oncogene* 1996; **13**: 1621–1630.
24 Davies BR, Davies MP, Gibbs FE, Barraclough R, Rudland PS. Induction of the metastatic phenotype by transfection of a benign rat mammary epithelial cell line with the gene for p9Ka, a rat calcium-binding protein, but not with the oncogene EJ-ras-1. *Oncogene* 1993; **8**: 999–1008.
25 Grigorian M, Ambartsumian N, Lykkesfeldt AE, Bastholm L, Elling F, Georgiev G *et al.* Effect of mts1 (S100A4) expression on the progression of human breast cancer cells. *Int J Cancer* 1996; **67**: 831–841.
26 Chen H, Fernig DG, Rudland PS, Sparks A, Wilkinson MC, Barraclough R. Binding to intracellular targets of the metastasis-inducing protein, S100A4 (p9Ka). *Biochem Biophys Res Commun* 2001; **286**: 1212–1217.
27 Fernandez-Fernandez MR, Veprintsev DB, Fersht AR. Proteins of the S100 family regulate the oligomerization of p53 tumor suppressor. *Proc Natl Acad Sci USA* 2005; **102**: 4735–4740.
28 Grigorian M, Andresen S, Tulchinsky E, Kriajevska M, Carlberg C, Kruse C *et al.* Tumor suppressor p53 protein is a new target for the metastasis-associated Mts1/S100A4 protein: functional consequences of their interaction. *J Biol Chem* 2001; **276**: 22699–22708.
29 Ismail TM, Zhang S, Fernig DG, Gross S, Martin-Fernandez ML, See V *et al.* Self-association of calcium-binding protein S100A4 and metastasis. *J Biol Chem* 2010; **285**: 914–922.
30 van Dieck J, Fernandez-Fernandez MR, Veprintsev DB, Fersht AR. Modulation of the oligomerization state of p53 by differential binding of proteins of the S100 family to p53 monomers and tetramers. *J Biol Chem* 2009; **284**: 13804–13811.
31 van Dieck J, Teufel DP, Jaulent AM, Fernandez-Fernandez MR, Rutherford TJ, Wyslouch-Cieszynska A *et al.* Posttranslational modifications affect the interaction of S100 proteins with tumor suppressor p53. *J Mol Biol* 2009; **394**: 922–930.
32 Berge G, Maelandsmo GM. Evaluation of potential interactions between the metastasis-associated protein S100A4 and the tumor suppressor protein p53. *Amino Acids* 2011; **41**: 863–873.
33 Orre LM, Pernemalm M, Lengqvist J, Lewensohn R, Lehtio J. Up-regulation, modification, and translocation of S100A6 induced by exposure to ionizing radiation revealed by proteomics profiling. *Mol Cell Proteomics* 2007; **6**: 2122–2131.
34 Vassilev LT, Vu BT, Graves B, Carvajal D, Podlaski F, Filipovic Z *et al. In vivo* activation of the p53 pathway by small-molecule antagonists of MDM2. *Science* 2004; **303**: 844–848.
35 Soderberg O, Leuchowius KJ, Gullberg M, Jarvius M, Weibrecht I, Larsson LG *et al.* Characterizing proteins and their interactions in cells and tissues using the in situ proximity ligation assay. *Methods* 2008; **45**: 227–232.
36 van Dieck J, Lum JK, Teufel DP, Fersht AR. S100 proteins interact with the N-terminal domain of MDM2. *FEBS Lett* 2010; **584**: 3269–3274.
37 Sali A, Glaeser R, Earnest T, Baumeister W. From words to literature in structural proteomics. *Nature* 2003; **422**: 216–225.
38 Vasilescu J, Guo X, Kast J. Identification of protein-protein interactions using *in vivo* cross-linking and mass spectrometry. *Proteomics* 2004; **4**: 3845–3854.
39 Deshaies RJ, Joazeiro CA. RING domain E3 ubiquitin ligases. *Annu Rev Biochem* 2009; **78**: 399–434.
40 Kim JH, Kim CN, Kim SY, Lee JS, Cho D, Kim JW *et al.* Enhanced S100A4 protein expression is clinicopathologically significant to metastatic potential and p53 dysfunction in colorectal cancer. *Oncol Rep* 2009; **22**: 41–47.
41 Berge G, Costea DE, Berg M, Rasmussen H, Grotterod I, Lothe RA *et al.* Coexpression and nuclear colocalization of metastasis-promoting protein S100A4 and p53 without mutual regulation in colorectal carcinoma. *Amino Acids* 2011; **41**: 875–884.
42 Tang Y, Zhao W, Chen Y, Zhao Y, Gu W. Acetylation is indispensable for p53 activation. *Cell* 2008; **133**: 612–626.
43 Hjerpe R, Aillet F, Lopitz-Otsoa F, Lang V, Torres-Ramos M, Farras R *et al.* Oligomerization conditions Mdm2-mediated efficient p53 polyubiquitylation but not its proteasomal degradation. *Int J Biochem Cell Biol* 2010; **42**: 725–735.
44 Katayama H, Sasai K, Kawai H, Yuan ZM, Bondaruk J, Suzuki F *et al.* Phosphorylation by aurora kinase A induces Mdm2-mediated destabilization and inhibition of p53. *Nat Genet* 2004; **36**: 55–62.
45 Shieh SY, Ikeda M, Taya Y, Prives C. DNA damage-induced phosphorylation of p53 alleviates inhibition by MDM2. *Cell* 1997; **91**: 325–334.

46 van Dieck J, Brandt T, Teufel DP, Veprintsev DB, Joerger AC, Fersht AR. Molecular basis of S100 proteins interacting with the p53 homologs p63 and p73. *Oncogene* 2010; **29**: 2024–2035.
47 Itahana Y, Ke H, Zhang Y. p53 Oligomerization is essential for its C-terminal lysine acetylation. *J Biol Chem* 2009; **284**: 5158–5164.
48 Poyurovsky MV, Katz C, Laptenko O, Beckerman R, Lokshin M, Ahn J *et al.* The C terminus of p53 binds the N-terminal domain of MDM2. *Nat Struct Mol Biol* 2010; **17**: 982–989.
49 Brooks CL, Gu W. p53 ubiquitination: Mdm2 and beyond. *Mol Cell* 2006; **21**: 307–315.
50 Sherr CJ. Divorcing ARF and p53: an unsettled case. *Nat Rev Cancer* 2006; **6**: 663–673.
51 De Petris L, Orre LM, Kanter L, Pernemalm M, Koyi H, Lewensohn R *et al.* Tumor expression of S100A6 correlates with survival of patients with stage I non-small-cell lung cancer. *Lung Cancer* 2009; **63**: 410–417.
52 Kaminskyy VO, Piskunova T, Zborovskaya IB, Tchevkina EM, Zhivotovsky B. Suppression of basal autophagy reduces lung cancer cell proliferation and enhances caspase-dependent and -independent apoptosis by stimulating ROS formation. *Autophagy* 2012; **8**: 1032–1044.

Supplementary Information accompanies this paper on the Oncogene website (http://www.nature.com/onc)